Riset Geologi dan Pertambangan
Earth science journal · Open access · BRIN Earth Sciences & Maritime · BRIN Publishing
ISSN 0125-9849 e-ISSN 2354 6638

RESEARCH ARTICLE
OPEN ACCESS

Riset Geologi dan Pertambangan (2026) Vol. 36, No. 1, 73–84
DOI: 10.55981/risetgeotam.2026.1410

Keywords:
Squeezing
Squeezing pressure
Support pressure
Deep tunnel

Corresponding author:
Farrel Rheza Prakusya
rhezafarrel@gmail.com

Article history:
Received : 15 June 2025
Revised : 10 September 2025
Accepted : 12 November 2025

Author Contributions:
Conceptualization: FRP
Data curation: FRP, SHP
Formal analysis: FRP, SHP
Funding acquisition: FRP, SHP
Investigation: FRP, SHP
Methodology: FRP, SHP, RKW
Supervision: SHP, RKW
Visualization: FRP, SHP
Writing – original draft: FRP, SHP
Writing – review & editing: RKW

Citation:
Prakusya, F. R., Prasetyo, S. H., Wattimena, R., K., 2026. Numerical analysis to determine squeezing potential of deep tunnel. J. Ris. Geol. Pertamb., 36 (1), 73–84, doi: 10.55981/risetgeotam.2026.1410

Numerical analysis to determine squeezing potential of deep tunnel

Farrel Rheza Prakusya, Simon Heru Prassetyo, Ridho Kresna Wattimena

Department of Mining Engineering, Institut Teknologi Bandung (ITB)
Jalan Ganesa No.10, Bandung, 40132, Indonesia

Abstract

Squeezing refers to large, time-dependent deformations that happen around the tunnel perimeter. This phenomenon commonly occurs in tunnel excavations with poor rock mass class and very great depth. In many cases, squeezing exerts considerable pressure, which can damage the installed tunnel support system. In this study, numerical modeling was carried out on 10 tunnels in both squeezing and non-squeezing conditions based on data from the literature, using actual support pressure values to obtain modeled convergence values that match the observed ones. The results showed a difference between the numerical and actual convergence values that were due to additional pressure from squeezing. This squeezing pressure was then modeled by increasing the horizontal and vertical stresses until the numerical convergence matched the actual convergence. The effectiveness of this approach was confirmed by plastic zone validation in a selected case using the 2D FEM method. The final model successfully reflected real tunnel behavior, particularly in squeezing-prone zones. These results emphasize the importance of accurately modeling squeezing pressure to determine realistic deformation levels and develop appropriate support design.

1. Introduction

Excavating tunnels through poor-quality rock masses and at considerable depths often leads to challenges, one of the most common being squeezing, a time-dependent deformation that develops around the tunnel perimeter. This type of deformation generates substantial pressure on the tunnel structure, which can potentially damage the support systems that have been installed Barla (2001). Jethwa (1981), Goel et al. (1995), and Sakurai (1997) stated that when the deformation of an unsupported underground opening exceeds 1% of its span, the ground can be classified as squeezing. This situation is likely to cause construction difficulties. However, Singh et al. (2007) argued that the critical circumferential strain value beyond which problems may arise is not necessarily fixed at 1%, as it depends on the characteristics of the rock mass. If the installed support systems are insufficient, tunnel deformation in squeezing ground conditions may persist over an extended period (Jethwa, 1981).

Recent research has been seeking to improve the prediction and control of squeezing. Akbariforouz et al. (2022) demonstrated that geo-electrical resistivity data can provide a more accurate basis for predicting squeezing intensity by correlating resistivity with in-situ strain. In parallel, (Xie et al., 2025) highlighted that squeezing is inherently time-dependent and proposed active control measures to mitigate its progressive deformation. Field investigations in layered soft rock tunnels also showed that the performance of support systems such as cartridge rock bolts, steel floral pipes, lattice girders, and I-beams plays

a crucial role in controlling deformation under squeezing conditions (Chen et al., 2023) Complementing these findings, Claresta et al. (2022) proposed that maintaining an adequate ratio between support pressure and in-situ stress (pi/po) is key, recommending values of 0.4 for extreme squeezing and progressively lower ratios for less severe cases.

Squeezing may occur when the support pressure provided by the installed support system is lower than the estimated required support pressure. Conversely, squeezing is unlikely to happen if the applied support pressure is equal to or greater than the estimated requirement. Typically, squeezing is associated with strain values that exceed the critical strain threshold of the rock mass. This condition can arise due to additional stresses induced by the squeezing itself that result in strain levels that surpass the rock mass's critical limit. One such squeezing incident occurred in the headrace tunnel of the Chameliya Hydroelectric Project (CHEP) (Figure 1), where tunnels excavated through phyllite and limestone under high overburden stress experienced extreme squeezing deformation (Basnet, 2013; Shrestha, 2021).

Figure 1. Squeezing at Chameliya Hydroelectric Project Headrace Tunnel (CHEP) (Basnet, 2013)

2. Data and methods

The data utilized in this study are derived from 10 tunnel case histories encompassing both squeezing and non-squeezing conditions. These datasets include parameters such as rock strength, actual strain obtained from convergence measurements, tunnel span dimensions, depth, and the applied support pressure values. The data is presented in Table 1.

Table 1. Tunnel data cases used in this study

No	Name of Tunnel	Location	a (m)	H (m)	σ_{cm} (MPa)	ε (%)	p_{smax} (MPa)	Squeezing category	References
1	Kaletape Section 2	Turkey	6.3	52	15.32	0.08	0.54	Non-squeezing	Singh et al. (1992)
2	Kaletape Section 3	Turkey	6.3	215	34.79	0.12	0.54	Non-squeezing	Singh et al. (1992)
3	Maneri stage II	India	3.5	415	7.25	2.19	0.29	Minor	Baburao (2007)
4	Maneri stage II	India	3.5	510	7.24	2.42	0.29	Minor	Baburao (2007)
5	Golab Tunnel - Sec 4	Iran	2.3	240	2.9	3.85	0.48	Severe	Akbariforouz et al. (2022)
6	Golab Tunnel - Sec 6	Iran	2.3	160	2.1	2.80	0.48	Severe	Akbariforouz et al. (2022)
7	Giri-Bata tunnel	India	2.3	200	2.96	6.20	0.17	Very severe	Goel et al. (1995)
8	Giri-Bata tunnel	India	2.3	400	4.02	7.61	0.17	Very severe	Goel et al. (1995)
9	Chameliya Ch. 3 + 733	Nepal	2.7	238	2.2	10.96	0.66	Extremely severe	Basnet (2013)
10	Chameliya Ch. 3 + 296	Nepal	2.7	252	2.2	12.50	0.64	Extremely severe	Basnet (2013)

Squeezing Prediction According to Hoek and Marinos (2000)**.**

Hoek & Marinos (2000) conducted a comprehensive analysis that indicated that the ratio between rock mass strength (σ_{cm}) and in-situ stress (p_o) can be used to estimate tunnel deformation. They applied closed-form solution equations for circular tunnels under hydrostatic stress conditions to compute strain values and performed Monte Carlo simulations across a range of tunnel scenarios, considering variations in in-situ stress, tunnel diameter, depth, and rock mass strength in unsupported tunnel conditions (Figure 2).

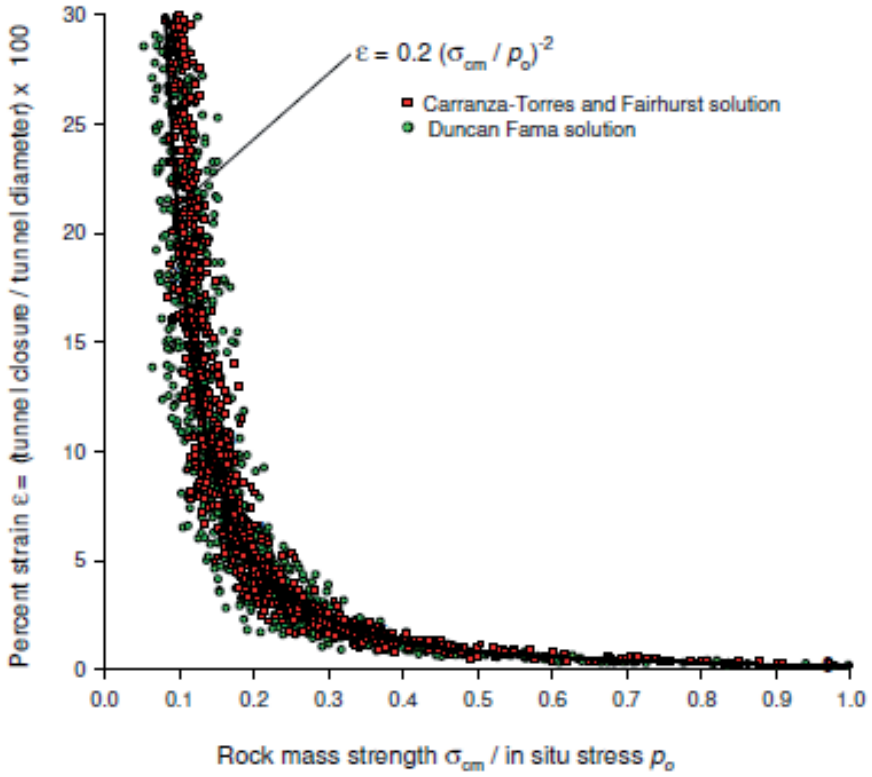

Figure 2. Plot of tunnel convergence against the ratio of rock mass strength to in-situ stress (Hoek & Marinos, 2000)

Hoek & Marinos (2000) refined their analysis by modeling the internal support pressure (p_i) to account for the role of support systems in tunnels. They applied data-fitting techniques to generate a formula that can be used to evaluate both the development of the plastic zone and the deformation behavior of tunnels in squeezing ground conditions (Eq. 1). Using this formula, various levels of squeezing were classified as functions of tunnel strain, as illustrated in Figure 3.

$$\frac{\delta_i}{d_0} = \left(0.002 - 0.0025\,\frac{p_i}{p_0}\right)\frac{\sigma_{cm}}{p_0}^{\left(2.4\frac{p_i}{p_0}-2\right)} \quad (1)$$

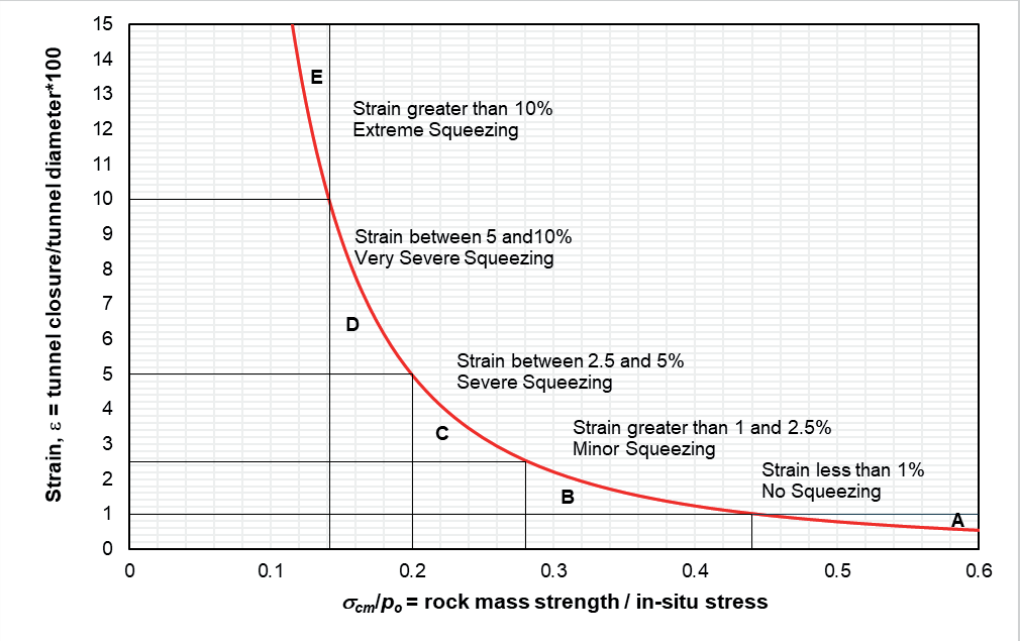

Figure 3. Relationship between strain at the tunnel wall (ε), rock mass strength (σ_{cm}), and in-situ stress (p_0) (Hoek & Marinos, 2000)

Squeezing Pressure

Jethwa (1981) explained that squeezing pressure is the force generated by the plastic deformation of rock around a tunnel, caused by an imbalance between in-situ stress and rock strength. This occurs when the surrounding rock weakens due to specific geological conditions, such as excessive stress in deeper layers and low rock mass strength. (Jethwa, 1981) developed an empirical approach to evaluate and predict squeezing pressure based on the ratio of in-situ stress to rock strength, along with other geotechnical factors like rock deformation modulus and local geological properties. This method aids in determining the appropriate tunnel support design to manage or mitigate the effects of squeezing.

3. Results

A numerical analysis was performed on 10 tunnel cases to investigate a range of squeezing conditions, from non-squeezing to extreme squeezing. The urgency of this study lies in the need to understand and predict the behavior of rock masses surrounding tunnels under squeezing conditions, particularly in projects located in areas with high in-situ stress and plastic rock properties. The purpose of the numerical analysis on the tunnel models is to verify whether the numerical convergence results correspond to the actual field conditions. The analysis was carried out through the following steps:

Step 1. Model dimensions and rock properties. The tunnel construction simulation is carried out using the Finite Element Method (FEM) implemented in the RS2 software. The tunnel diameter and rock properties are adjusted according to the tunnel conditions to be analyzed (Table 2). The geometric shape of the tunnel and the mesh network used are shown in Figure 4, which is an example of the Giri-Bata tunnel at a depth of 400 m.

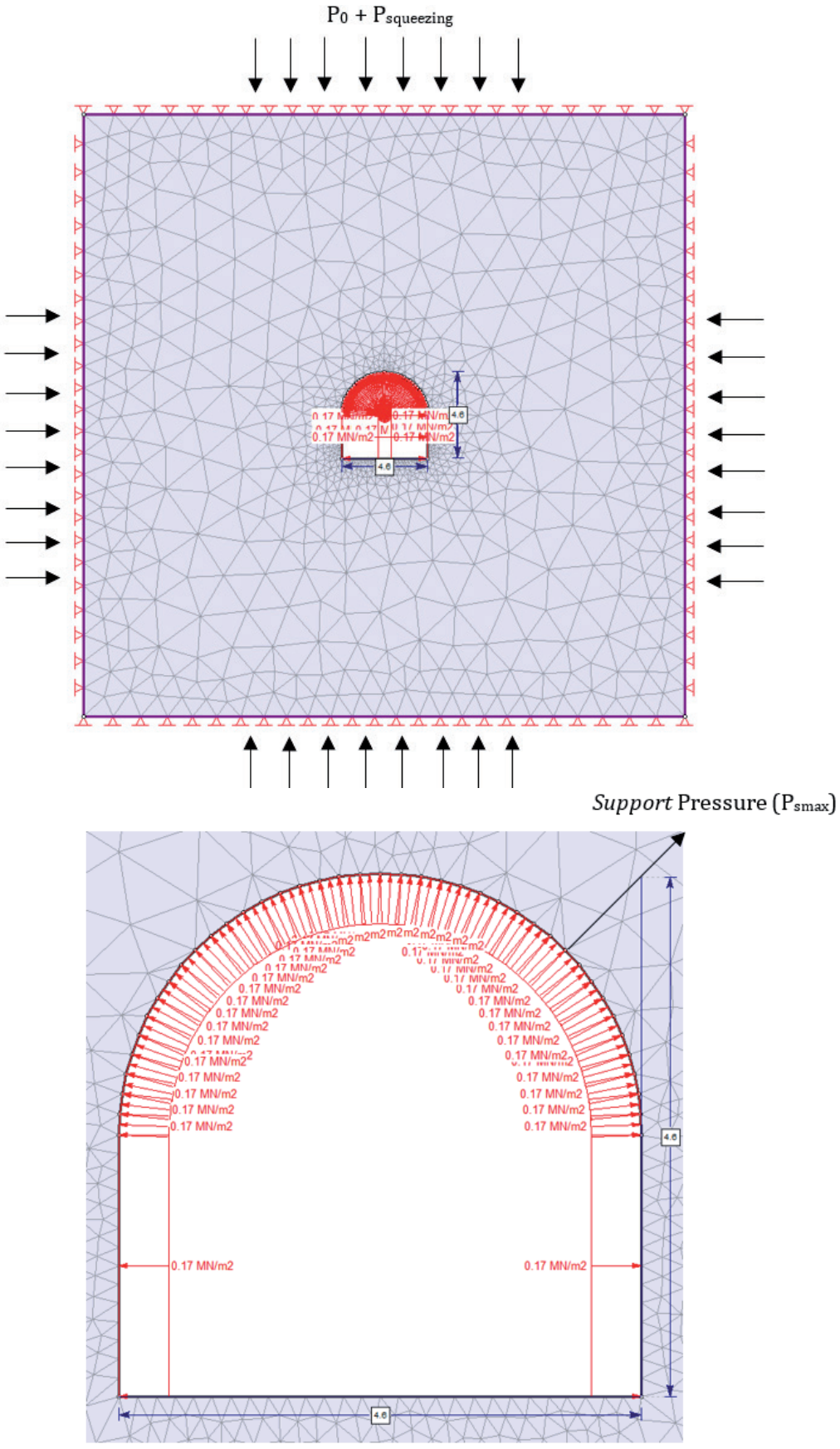

Figure 4. FEM model with support pressure (pi) Giri-Bata tunnel at a depth of 400 m

Table 2. Material properties used in the numerical modeling

No	Tunnel	σ_{ci} (MPa)	m_i	E_i (MPa)	v	g (t/m^3)	GSI	mb	s	a
1	Kaletape Section 2	72.00	9	20007	0.1	2.68	40	0.516	3.3E-04	0.511
2	Kaletape Section 3	90.00	9	31942	0.1	2.69	52	0.915	1.6E-03	0.504
3	Maneri stage II	50.00	18	18013	0.1	2.50	34	0.620	1.1E-04	0.517
4	Maneri stage II	50.00	18	18013	0.1	2.50	34	0.630	1.1E-04	0.516
5	Golab Tunnel - Sec 4	18.70	6	9700	0.1	2.74	74	1.592	2.7E-02	0.500
6	Golab Tunnel - Sec 6	8.00	6	3600	0.1	2.75	68	1.172	1.1E-02	0.501
7	Giri-Bata tunnel	85.50	4	7211	0.1	2.30	15	0.052	7.4E-06	0.561
8	Giri-Bata tunnel	85.50	4	7211	0.1	2.30	15	0.052	7.4E-06	0.561
9	Chameliya Ch. 3 + 733	39.00	8	7211	0.1	2.80	15	0.327	5.7E-06	0.561
10	Chameliya Ch. 3 + 296	39.00	8	7211	0.1	2.80	15	0.327	5.7E-06	0.561

Step 2. Establish initial equilibrium. Stresses are initialized using gravity. The horizontal-to-vertical stress ratio is 1. In this model, fixed-support boundary conditions are applied to ensure stability and restrict movement at specific points.

Step 3. Set up the Mesh. Set up a graded mesh with 3-node triangular elements.

Step 4. Install supports on the model to reinforce the structure. The supports are calibrated according to the maximum strength values of the actual supports, represented in the form of loads.

Step 5. Perform the numerical analysis. In the initial analysis, we evaluate whether the numerical convergence values correspond to the actual convergence values. Figure 5 shows the initial numerical convergence values, which do not yet correspond to the actual convergence values.

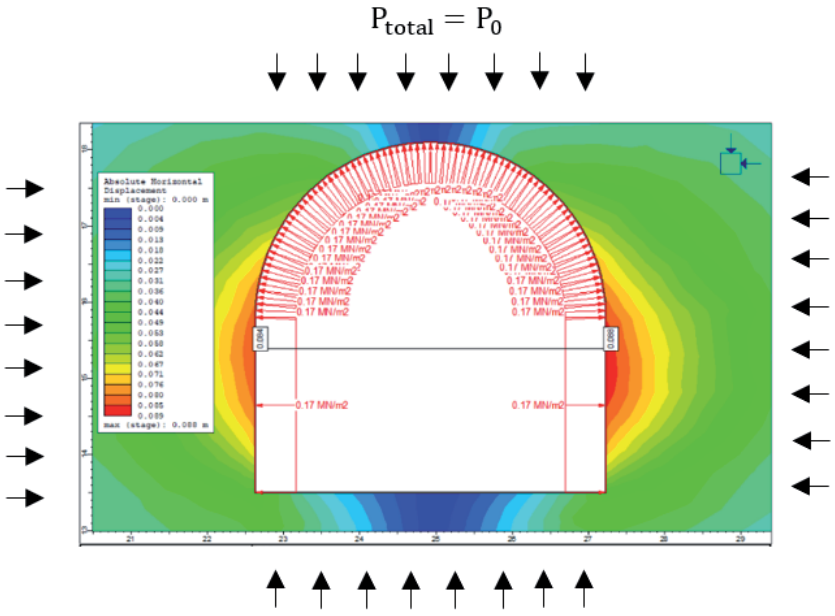

Figure 5. FEM model result for the Giri-Bata tunnel at a depth of 400 m before the addition of squeezing pressure.

Step 6. Evaluate the initial model. The initial model evaluation is performed by incrementally increasing the horizontal and vertical stress values up to a defined limit. This approach aims to simulate the squeezing pressure experienced by the tunnel, ensuring that the numerical convergence values accurately represent the actual convergence conditions. In the initial stage of the numerical simulation, squeezing pressure was applied based on estimated in-situ stress conditions. As shown in Figure 6, the resulting numerical convergence values had not yet aligned with the actual field measurements, indicating that the applied stress input did not fully capture the real tunnel behavior. To improve the model accuracy, the in-situ stress values were incrementally increased. The subsequent analysis, presented in Figure 7, shows that the numerical convergence values closely matched the observed field data. This agreement validates the model's ability to simulate the actual ground response and confirms that the adjusted stress conditions better represent the true in-situ environment.

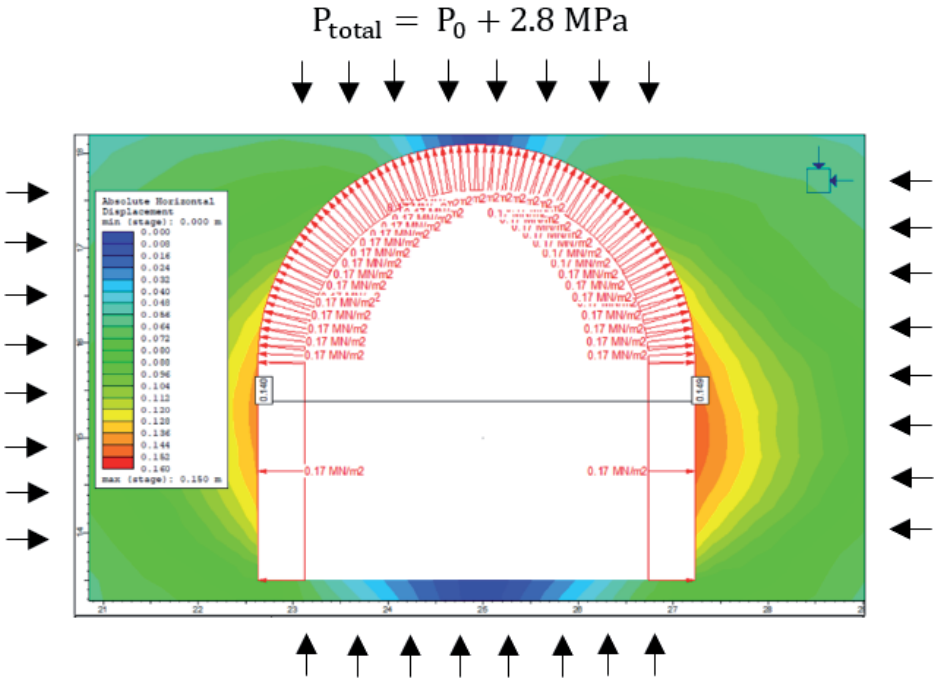

Figure 6. FEM model result for the Giri-Bata tunnel at a depth of 400 m after the first squeezing pressure application.

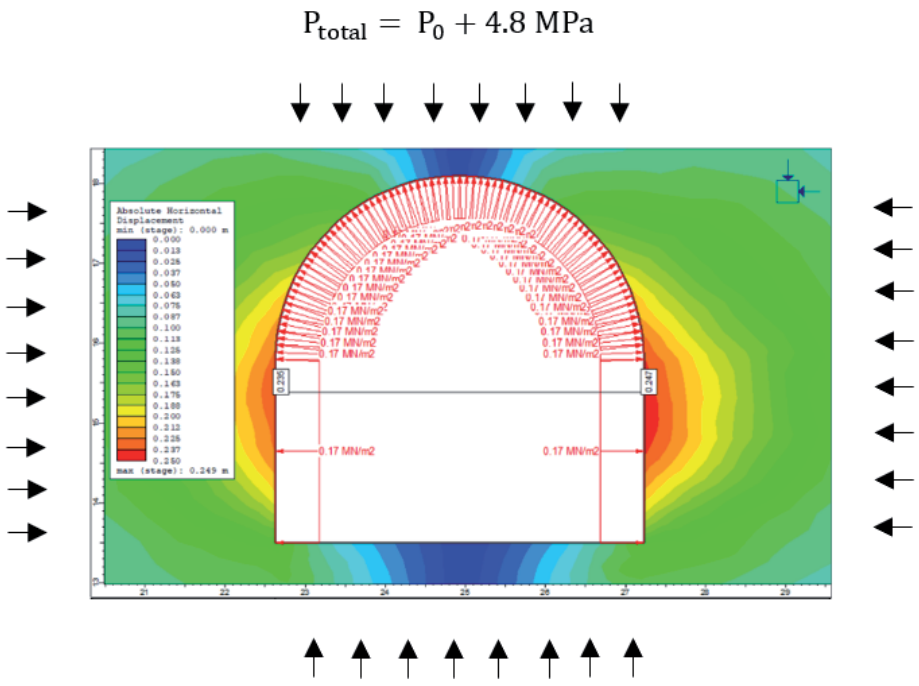

Figure 7. FEM model result for the Giri-Bata tunnel at a depth of 400 m after the second squeezing pressure application.

Step 7. Calculate the value of squeezing pressure. After the model evaluation was conducted until the numerical convergence matched the actual field measurements, the squeezing pressure could be determined. The value of the squeezing pressure can be calculated using Eq. (2) and (3):

$$p_{total} = p_0 + p_{squeezing} \quad (2)$$

$$p_{squeezing} = p_{total} - p_0 \quad (3)$$

In the numerical models presented in Figures 5, 6, and 7, the squeezing pressure was applied by incrementally increasing both vertical and horizontal in-situ stresses along the tunnel boundary. This method was adopted to simulate the additional load resulting from time-dependent deformation of the surrounding rock mass under squeezing conditions. The convergence values of the model examples are presented in Table 3 below.

Table 3. Comparison of Numerical Model Outcomes: Without and With Squeezing Pressure

Model	P_{smax} (MPa)	P_0 (MPa)	$P_{Squeezing}$ (MPa)	P_{total} (MPa)	Convergence (cm)
Without Squeezing Pressure	0.17	9.20	0.00	9.20	17.20
With Squeezing Pressure (1)	0.17	9.20	2.80	12	28.90
With Squeezing Pressure (2)	0.17	9.20	4.80	14.00	47.00

The recap of the numerical modeling simulation results is presented in Table 4, which shows the required squeezing pressure values needed to achieve convergence values that match the actual tunnel convergence.

Table 4. Modeling results using squeezing pressure and actual support pressure to obtain simulated convergence that matches actual convergence

No	Tunnel	H (m)	σ_v (MPa)	Squeezing Pressure (MPa)	Support Pressure (MPa)	Modeled Convergence (cm)	Actual Convergence (cm)
1	Kaletape Section 2	225	1.39	6.61	0.54	1.00	1.00
2	Kaletape Section 3	138	5.78	11.22	0.54	1.80	1.50
3	Maneri stage II	415	10.38	13.12	0.29	15.40	15.30
4	Maneri stage II	510	10.00	26.00	0.29	16.70	16.70
5	Golab Tunnel - Sec 4	240	6.58	40.42	0.48	17.80	17.80
6	Golab Tunnel - Sec 6	160	4.40	9.70	0.48	12.80	12.80
7	Giri-Bata tunnel	200	4.60	5.20	0.17	28.50	28.50
8	Giri-Bata tunnel	400	9.20	4.80	0.17	47.00	47.00
9	Chameliya Ch. 3 + 733	238	6.66	20.34	0.66	59.00	59.00
10	Chameliya Ch. 3 + 296	252	7.00	21.50	0.64	67.50	67.50

4. Discussion

Ten tunnel cross-sections were selected as representative models to be analyzed in this study. To obtain numerical convergence results that reflect actual conditions caused by the squeezing phenomenon, squeezing pressure was simulated by increasing both the horizontal and vertical stresses in the model. It is important to note that squeezing pressure was not applied in the model with the original initial support design, and therefore the resulting structural response does not fully represent the actual behavior under squeezing conditions observed in the field.

The application of squeezing pressure in the numerical model is based on the results of preliminary simulations which showed that, without the inclusion of squeezing effects, the calculated numerical convergence did not match the field measurements. According to (Jethwa, 1981), squeezing pressure refers to the pressure generated by the plastic deformation of the rock mass surrounding a tunnel, which occurs due to an imbalance between the in-situ stress and the rock strength. This pressure acts on the installed support system and can significantly affect its performance. Therefore, in order to better replicate the actual tunnel behavior under squeezing conditions, additional squeezing pressure was introduced in the model by increasing the horizontal and vertical stresses acting on the tunnel boundary.

Table 4 above demonstrates that the method of incorporating squeezing pressure is sufficiently effective in simulating the squeezing phenomenon observed in deep tunnels. As shown in Figure 7 above, the tunnel convergence obtained from the numerical simulation closely matches the actual measured convergence, indicating that this modeling approach is valid and appropriate for the present study.

The numerical simulation results for the Chameliya Tunnel at Ch. 3+733, which is classified as being under extreme squeezing conditions, indicate that the original support design was unable to withstand the ground pressure surrounding the tunnel. As a result, excessive deformation occurred, with tunnel convergence reaching 67.5 cm or approximately 10.96% strain. This finding highlights the need for more effective alternative support systems to control deformation and ensure tunnel stability. Furthermore, other tunnels classified as being under minor, severe, very severe, or extreme squeezing conditions should also be carefully evaluated and provided with appropriate alternative support recommendations to mitigate the potential for excessive squeezing-related deformations.

In comparison, the analysis of the Golab Tunnel – Sec 4 and the Chameliya Ch. 3+296 Tunnel reveals that, despite being subjected to higher squeezing pressure, the Golab Tunnel – Sec 4 exhibits lower convergence. This is attributed to differences in the mechanical properties of the rock mass, as shown in Table 2, where the Golab Tunnel – Sec 4 has a higher modulus of elasticity (E) and Geological Strength Index (GSI) compared to Chameliya Ch. 3+296. With a stiffer rock mass, a larger additional squeezing pressure is required in the numerical simulation to produce convergence values that match the actual field measurements.

Validation of the simulated squeezing pressure in the 2D FEM model was carried out by observing the development of plastic zones before and after the application of squeezing pressure. This approach supports (Jethwa's, 1981) statement that squeezing pressure is generated by the plastic deformation of the rock surrounding a tunnel due to an imbalance between in-situ stress and rock strength. It is also important to acknowledge that squeezing is inherently a time-dependent phenomenon. In this case, only the final tunnel convergence data were available, without temporal measurements of deformation development. As such, the modeling approach adopted was static and based on the end-state conditions observed in the field. While time-dependent models such as creep simulations could potentially provide more realistic deformation behavior, their application was not feasible due to the lack of incremental or time-series data. Therefore, the static model presented here reflects the final deformation condition as a practical approximation of squeezing effects.

The model was developed using secondary data from the Golab Tunnel Section 4. Numerical modeling was carried out using the Generalized Hoek-Brown failure criterion. The presence of plastic zones confirmed the expected behavior. Table 5 presents the material properties used in the numerical simulation. The numerical simulation results are shown in Figure 8 and Figure 9. Figure 9 shows that the plastic zone appears when squeezing pressure is applied to the model.

Table 5. Material Properties in the Numerical Model for Squeezing Pressure Validation

Parameter	Value
Name of tunnel	Golab-Tunnel Sec 4
Rock type	Shale
σ_{ci} (MPa)	18.7
mi	6
Ei (MPa)	9700
v	0,1
γ (t/m^3)	2.5
p_0 (MPa)	6.58
GSI	74
mbmb	1.59238
s	2.70E-02
a	0.5

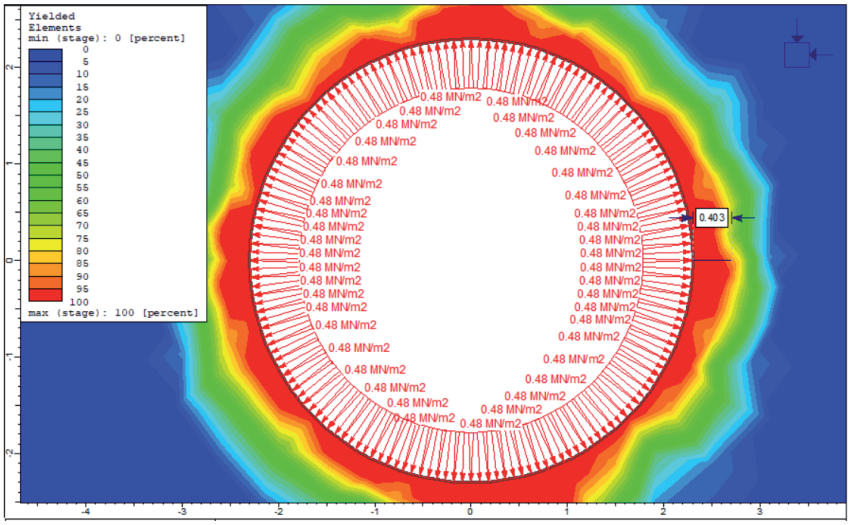

Figure 8. Yield element value of the tunnel without squeezing pressure.

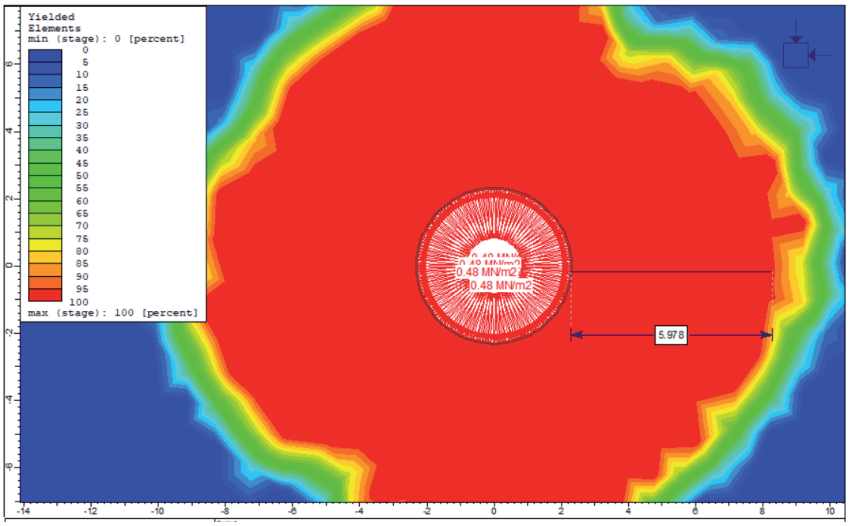

Figure 9. Yield element value of the tunnel with squeezing pressure.

As shown in Table 6, the plastic zone begins to develop when the squeezing pressure is introduced into the model.

Table 6. Comparison of Tunnel Yield Elements With and Without Squeezing Pressure

Model	Support Pressure (MPa)	σ_v (MPa)	Plastic Zone (m)
Without Squeezing Pressure	0.48	6.58	0.403
With Squeezing Pressure	0.48	47.00	5.978

The squeezing pressure corresponding to this condition was calculated as follows:

$$p_{squeezing} = p_{total} - p_0$$

$$p_{squeezing} = 47 - 6.58$$

$$p_{squeezing} = 40.42$$

This observation is consistent with the findings of Jethwa (1981), who stated that the pressure generated by the plastic deformation of the rock mass surrounding the tunnel arises as a response to the imbalance between the in-situ stress and the rock strength.

5. Conclusions

This study employed numerical modeling on ten tunnel cases under various squeezing classifications, from non-squeezing to extreme squeezing conditions. The methodology involved applying additional squeezing pressure by incrementally increasing both horizontal and vertical in-situ stresses in the FEM simulation until the numerical convergence matched the actual field measurements. Model validity was confirmed through plastic zone analysis, which aligned with field observations.

The results showed that each squeezing classification corresponded to a distinct squeezing pressure value influenced by the geological and geomechanical properties of the surrounding rock mass. For example, despite experiencing higher squeezing pressure, the Golab Tunnel – Sec 4 exhibited lower convergence than the Chameliya Ch. 3+296 Tunnel due to its higher modulus of elasticity and GSI, which indicate a stiffer rock mass. In cases such as the Chameliya Tunnel at Ch. 3+733, the original support design proved inadequate, resulting in excessive deformation with convergence reaching 67.5 cm (10.96% strain).

These findings have significant technical implications. For tunnels classified under moderate to extreme squeezing conditions, the original support systems are often insufficient to control deformation. Therefore, adaptive and more effective alternative support designs capable of accommodating higher squeezing pressures are recommended to ensure long-term tunnel stability and safety in similar geological environments.

Acknowledgments

The authors would like to express their sincere gratitude to the Department of Mining Engineering at the Institut Teknologi Bandung (ITB) for the academic and technical support provided throughout this research. The authors are also thankful to the researchers and authors whose data and case studies were referenced in this study. This research was conducted independently and did not receive funding from any government, private, or non-profit agency. This research is funded by the Institut Teknologi Bandung Excellence Research Program 2026 (Contract No. 2235/IT1.B07.1/TA.00/2026).

References

Akbariforouz, M., Taherdangkoo, R., Baghbanan, A., Butscher, C., 2022. Prediction of Tunnel Squeezing in Soft Sedimentary Rocks by Geo-electrical Data. Res. Sq. https://doi.org/10.21203/rs.3.rs-1345549/v1

Baburao, C.J., 2007. Closure of Underground Openings in Jointed Rocks (Ph.D. Thesis). Indian Institute of Technology Roorkee. http://shodhbhagirathi.iitr.ac.in:8081/jspui/handle/123456789/1597

Barla, G., 2001. Tunnelling under squeezing rock conditions. In: Kolymbas, D. (Ed.), Tunnelling Mechanics - Advances in Geotechnical Engineering and Tunnelling, pp. 169–268.

Basnet, C.B., 2013. Evaluation on the Squeezing Phenomenon at the Headrace Tunnel of Chameliya Hydroelectric Project, Nepal (Master's Thesis). Norwegian University of Science and Technology. https://brage.bibsys.no/xmlui/handle/11250/236161

Chen, Y., Li, Z., Cui, T., 2023. Field Investigation of the Reinforcement and Support Mechanism for a Tunnel in Layered Soft Rock Mass. KSCE J. Civ. Eng. 27, 4534–4543. https://doi.org/10.1007/s12205-023-0668-x

Claresta, A., Prassetyo, S.H., Wattimena, R.K., 2022. Analysis of support pressure requirement to minimize squeezing potential in deep tunnels. In: Proc. Int. Symp. Earth Sci. Technol. 2022, Fukuoka, Japan, pp. 474–479.

Goel, R.K., Jethwa, J.L., Paithankar, A.G., 1995. Tunnelling through the young Himalayas-A case history of the Maneri-Uttarkashi power tunnel. Eng. Geol. 39, 31–44. https://doi.org/10.1016/0013-7952(94)00002-j

Hoek, E., Marinos, P., 2000. Predicting Tunnel Squeezing Problems in Weak Heterogeneous Rock Masses. Tunnels Tunn. Int. 32, 45–51.

Jethwa, J.L., 1981. Evaluation of Rock Pressures in Tunnels Through Squeezing Ground in Lower Himalayas. (Ph.D. Thesis). University of Roorkee.

Sakurai, S., 1997. Lessons Learned from Field Measurements in Tunnelling. Tunn. Undergr. Sp. Technol. 12, 453–460.

Shrestha, N., 2021. Squeezing of Hydropower Tunnel from Nepal Lesser Himalaya. Sci. Eng. Technol. 1.

Singh, B., Jethwa, J.L., Dube, A.K., Singh, B., 1992. Correlation Between Observed Support Pressure and Rock Mass Quality. Tunn. Undergr. Sp. Technol. 7, 149–158. https://doi.org/10.1016/0886-7798(92)90114-W

Singh, M., Singh, B., Choudhari, J., 2007. Critical strain and squeezing of rock mass in tunnels. Tunn. Undergr. Sp. Technol. 22, 343–350. https://doi.org/10.1016/j.tust.2006.06.005

Xie, Z., He, C., Chen, Z., Zou, Y., Zhou, Y., Gu, H., 2025. Time-Dependent Squeezing Deformation Mechanism and Its Active Control Method of Deep Soft-Rock Tunnels Crossing Thrust Faults. Rock Mech. Rock Eng. 58, 2661–2687. https://doi.org/10.1007/s00603-024-04328-0